NEOPLASIA
www.neoplasia.com

Volume 16 Number 5 May 2014 pp. 403–412 403

A Small-Molecule Inhibitor of PIM Kinases as a Potential Treatment for Urothelial Carcinomas[1]

Jason M. Foulks*, Kent J. Carpenter†, Bai Luo*, Yong Xu*, Anna Senina*, Rebecca Nix*, Ashley Chan*, Adrianne Clifford*, Marcus Wilkes*, David Vollmer*, Benjamin Brenning*, Shannon Merx*, Shuping Lai*, Michael V. McCullar*, Koc-Kan Ho*, Daniel J. Albertson‡, Lee T. Call†, Jared J. Bearss§, Sheryl Tripp¶, Ting Liu‡, Bret J. Stephens†, Alexis Mollard†, Steven L. Warner†, David J. Bearss† and Steven B. Kanner*

*Astex Pharmaceuticals, Inc, Salt Lake City, UT; †Tolero Pharmaceuticals, Inc, Lehi, UT; ‡Department of Pathology, University of Utah School of Medicine, Salt Lake City, UT; §Huntsman Cancer Institute, University of Utah, Salt Lake City, UT; ¶ARUP Laboratories, Salt Lake City, UT

Abstract

The proto-oncogene proviral integration site for moloney murine leukemia virus (PIM) kinases (PIM-1, PIM-2, and PIM-3) are serine/threonine kinases that are involved in a number of signaling pathways important to cancer cells. PIM kinases act in downstream effector functions as inhibitors of apoptosis and as positive regulators of G_1-S phase progression through the cell cycle. PIM kinases are upregulated in multiple cancer indications, including lymphoma, leukemia, multiple myeloma, and prostate, gastric, and head and neck cancers. Overexpression of one or more PIM family members in patient tumors frequently correlates with poor prognosis. The aim of this investigation was to evaluate PIM expression in low- and high-grade urothelial carcinoma and to assess the role PIM function in disease progression and their potential to serve as molecular targets for therapy. One hundred thirty-seven cases of urothelial carcinoma were included in this study of surgical biopsy and resection specimens. High levels of expression of all three PIM family members were observed in both noninvasive and invasive urothelial carcinomas. The second-generation PIM inhibitor, TP-3654, displays submicromolar activity in pharmacodynamic biomarker modulation, cell proliferation studies, and colony formation assays using the UM-UC-3 bladder cancer cell line. TP-3654 displays favorable human ether-à-go-go-related gene and cytochrome P450 inhibition profiles compared with the first-generation PIM inhibitor, SGI-1776, and exhibits oral bioavailability. *In vivo* xenograft studies using a bladder cancer cell line show that PIM kinase inhibition can reduce tumor growth, suggesting that PIM kinase inhibitors may be active in human urothelial carcinomas.

Neoplasia (2014) 16, 403–412

Abbreviations: PIM, proviral integration site for moloney murine leukemia virus; STAT, signal transducer and activator of transcription; FLT3, fms-like tyrosine kinase 3; *hERG*, *human ether-à-go-go-related gene*; AML, acute myeloid leukemia; BAD, Bcl-2 associated death promoter.

Correspondence: David J. Bearss, PhD, Tolero Pharmaceuticals, Inc, Suite 320, 2975 W Executive Pkwy, Lehi, UT 84043. E-mail: dbearss@toleropharma.com

[1] Financial support: None of the above authors have been funded by any National Institutes of Health (NIH) or other applicable grants for this research. The research was funded independently by Astex Pharmaceuticals, Inc and Tolero Pharmaceuticals, Inc.

[2] This article refers to supplementary materials, which are available online at www.neoplasia.com.

Received 24 February 2014; Revised 12 May 2014; Accepted 13 May 2014

 1476-5586/14
http://dx.doi.org/10.1016/j.neo.2014.05.004

Introduction

The serine/threonine family of *proviral integration site for moloney murine leukemia virus* (*PIM*) *kinases* was first identified as proto-oncogenes activated in T cell lymphomas induced by murine leukemia viruses. The PIM kinase family comprises three members (PIM-1, PIM-2, and PIM-3) with six different isoforms from alternate translation-initiating sites [1–5]. Although the PIM kinase family is transcriptionally and translationally regulated in cells, these kinases lack a regulatory domain and are constitutively activated when expressed [6–10].

Expression of PIM-1 is induced by several cytokines, which often activate signal transducer and activator of transcription 5 (STAT5) in conjunction with PIM-1. In fact, the *PIM kinases* are target genes of STAT3 and STAT5 signaling and are correlated with levels of STAT signaling [11–15]. They often form complexes with heat shock protein 70 and Hsp90 for stabilization but are eventually polyubiquitinated for proteasomal degradation [11–15].

Although they are frequently implicated in acute myeloid leukemia (AML) [16], PIM kinases are overexpressed in many other types of hematological malignancies and solid tumors. Specifically, overexpression has been identified in bladder [17], prostate [18], and head and neck cancers [19] and chronic lymphocytic leukemia [20], multiple myeloma [21], and other B cell malignancies [22]. Overexpression of PIM kinases is often associated with poor prognosis in each of these cancers. For example, prostate tumors expressing high levels of PIM exhibited higher Gleason scores and differentiation [23]. Expression of Pim-1 has also been shown to predict poor prognosis in esophageal carcinoma [24] and gastric cancer [25].

The PIM kinases have a variety of downstream targets that are thought to contribute to tumor growth. In particular, PIM kinases target the proapoptotic B cell lymphoma 2–associated death promoter (BAD) family members and inhibit apoptosis [6–10]. Inhibition of PIM kinases has also been shown to decrease eukaryotic translation initiation factor 4E binding protein 1 (4EBP1) and cyclin D1 protein levels, suggesting a role for PIM kinases in translation and cell cycle regulation [26].

In addition to their role in apoptosis, PIM kinases have been shown to contribute to activation of oncogenic MYC signaling. PIM-1 phosphorylates serine 10 of histone H3 on the nucleosome of c-myc–binding sites, and this colocalization contributes to increased transcriptional activation of c-myc [27]. It has also been shown that overexpression of PIM-1 or PIM-2 stabilizes c-MYC by phosphorylation on Ser^{239} [28]. An *ex vivo* analysis of human prostate tumors showed that coexpression of PIM-1 and c-MYC is associated with higher Gleason scores [29]. PIM kinases are attractive therapeutic targets because of their clear role in inhibition of apoptosis, promotion of cell proliferation, and interactions with c-MYC [30].

Crystal structures of the PIM kinases have been used to understand their unique ATP binding pocket and for computational and medicinal chemistry efforts to develop inhibitors. The hinge region of PIM kinases is unusual in that it contains a proline residue not generally present in serine/threonine kinase hinges, as well as other unique residues in the ATP binding cleft [27,28,31–34]. Astex Pharmaceuticals, Inc (formerly SuperGen, Inc) (Salt Lake City, UT) developed an imidazopyridazine-based inhibitor, SGI-1776, that exhibited potent anti-PIM activity both *in vitro* and *in vivo* in a variety of preclinical models [35–38]. Studies have demonstrated that SGI-1776 exhibited potent antitumor activity in preclinical models of fms-like tyrosine kinase 3 (FLT3)-internal tandem duplication (ITD) mutant AML [38–40]. Investigators have demonstrated that the observed activity in this model system may be due to the predominant anti-FLT3 activity [41]. In contrast, models without the FLT3-internal tandem duplication (ITD) mutation were sensitive to SGI-1776, suggesting that PIM-specific activity may be responsible for the observed antiproliferative effects [42–47]. Ultimately, SGI-1776 was evaluated in a phase I clinical trial recruiting patients with either castration-resistant prostate cancer or relapsed/refractory non-Hodgkin lymphoma. However, the trial was terminated early due to a narrow therapeutic window, which resulted in cardiac QT prolongation. The cardiotoxicity has since been attributed to inhibition of the cardiac potassium channel *human ether-à-go-go-related gene* (hERG), also observed with SGI-1776 and related metabolites in functional assays.

Our recent efforts focused on identifying a novel PIM kinase inhibitor with a unique antikinase profile and attractive pharmaceutical properties. In this report, we describe the discovery and characterization of a second-generation small-molecule PIM kinase inhibitor, TP-3654 (SGI-9481), which exhibits potent activity against all three PIM kinases but with reduced activity against FLT3 and hERG.

The design of TP-3654 began with the virtual screening of a large number of library compounds, which identified pyrazolo[1,5-a]pyrimidines as active scaffolds against the PIM kinases. The pyrazolo[1,5-a] pyrimidine chemotype was of particular interest as the core structure was different from the imidazo[1,2- b]pyridazine compounds (SGI-1776), which were identified as selective and potent PIM inhibitors but with significant hERG and cytochrome P450 inhibition. Starting from this initial hit compound and SGI-1776, we combined the pyrazolo[1,5-a] pyrimidine core with the substituents at the 3,5-positions of SGI-1776 and generated a lead compound, which had an inhibition concentration 50% (IC_{50}) = 45 nM for PIM-1 kinase. On the basis of the structure of this lead compound, we conducted systematic modifications around this scaffold to improve *in vitro* potency against the PIM kinases, as well as other critical physicochemical properties. TP-3654 retains potent pan-PIM inhibition but with minimal to no hERG and cytochrome P450 inhibition as observed with SGI-1776.

PIM-1 has been observed in invasive and noninvasive urothelial carcinoma specimens, with a higher incidence in invasive cancer [17]. However, because the role of PIM kinases in bladder cancer is not well characterized, we sought to further evaluate PIM expression in low- and high-grade urothelial carcinoma. One hundred thirty-seven cases of urothelial carcinoma were included in this study of surgical biopsy and resection specimens. Furthermore, we evaluated the activity of TP-3654 in bladder cancer cell lines *in vitro* and in human xenograft mouse models. Overall, the data presented here provide preclinical activity to support the potential application of this inhibitor in urothelial carcinomas.

Materials and Methods

Synthesis of TP-3654

TP-3654 {4-((3-(3-(Trifluoromethyl)phenyl)imidazo[1,2-b]pyridazin-6-yl)amino) -*trans*-cyclohexyl)propan-2-ol} was prepared according to US Patent Application Publication US2012/0058997 (Imidazo[1,2-b]pyridazine and pyrazolo[1,5-A]pyrimidine derivatives and their use as protein kinase inhibitors).

PIM Kinase IC_{50} and K_i Determinations

PIM kinase K_i determinations, TP-3654 selectivity screens, and IC_{50} determinations were performed by Reaction Biology (Malvern,

PA). For K_i determination, PIM-1, PIM-2, or PIM-3 were incubated with 10-dose, three-fold serial dilutions of TP-3654 starting with 10 μM using five different concentrations of ATP (25, 50, 100, 250, and 500 μM ATP for PIM-1; 5, 10, 20, 50, and 100 μM ATP for PIM-2 and PIM-3), and the activity was measured at 0, 5, 10, 15, 20, 30, 45, 60, 75, 90, 105, and 120 minutes. The data were analyzed in a Michaelis-Menten plot to determine apparent K_m and K_i values using GraFit software (Erithacus Software, London, UK) using a mixed inhibition equation for global fit. For selectivity, 1 μM TP-3654 was tested against 336 kinases at a concentration of 10 μM ATP. IC_{50} determinations of phosphoinositide 3-kinase (PI3K) (α, β, δ, and γ) and all kinases inhibited by >50% from the initial screen were performed using 10-dose, three-fold serial dilutions of TP-3654 starting with 10 μM at K_m ATP concentrations for each kinase.

Cell Lines

The T24, RT4, J82, and UM-UC-3 bladder cancer cell lines were obtained directly from the American Type Culture Collection (ATCC) in Manassas, VA. These cell lines were passaged for less than 6 months before used in the described assays and were authenticated by ATCC. The MV4-11, PC-3, HEK-293, 22RV1, and NIH-3 T3 cells were obtained from ATCC but not authenticated by the authors.

hERG Assay

TP-3654 was tested for effect on hERG potassium channels by automated patch clamp method (QPatch^{HTX}, Sophion, Stockholm, Sweden) at WuXi AppTec (Shanghai, China). CHO cells stably expressing hERG potassium channels from Aviva Biosciences (San Diego, CA) were tested with TP-3654 at six concentrations, three-fold dilution starting at 30 μM with a final DMSO concentration of 0.15%, and compared to vehicle (negative) control and Amitriptyline (WuXi AppTec, Shanghai, China) (positive) controls. Percentage of control (vehicle) values was calculated in duplicate for each concentration of drug, and curve-fitting and IC_{50} calculations were performed by QPatch Assay Software (Sophion, Stockholm, Sweden).

Statistical Analysis and IC_{50}/effective concentration 50% (EC_{50}) Determination

Statistical analyses were performed by parametric analysis of variance test. IC_{50} and EC_{50} values were determined using GraphPad Prism software (La Jolla, CA).

Small hairpin RNA (shRNA) Transduction

UM-UC-3 cells (2.5×10^5) were seeded in a six-well plate in complete RPMI 1640 media and allowed to adhere overnight at 37°C in 5% CO_2. Cells were transduced with 8 μg/ml polybrene (Sigma-Aldrich, St. Louis, MI) and lentiviral particles at a multiplicity of infection of 50 based on titer values predetermined by Sigma-Aldrich using a p24 ELISA for each batch of shRNA. Following overnight transduction, viral-particle–containing media were removed and replaced with fresh complete media, and cells were cultured for an additional 48 hours at 37°C in 5% CO_2. Cells were trypsinized, and fractions of the transduced cells were collected for colony formation growth assays, whereas the remaining cells were collected for RNA and protein isolation.

Reverse Transcription–Polymerase Chain Reaction

RNA from 0.5×10^6 cells was isolated on a QIAcube (Qiagen, Santa Clarita, CA) using the protocol for purification of total RNA from animal cells (QIAshredder homogenization and on-column DNase digest) and quantified using a NanoDrop 8000 spectrophotometer (Thermo Electron, West Palm Beach, FL). Total RNA (1 μg) was converted to cDNA in a 20-μl reaction using the iScript cDNA synthesis kit (Bio-Rad Laboratories, Hercules, CA) by incubating the reaction components for 5 minutes at 25°C and 30 minutes at 42°C, followed by 5 minutes at 85°C. The cDNA reaction (2 μl) was used in a 20-μl polymerase chain reaction (PCR) multiplex reaction using 1X FAM-labeled PIM-1, VIC-labeled actin TaqMan primer sets, and the TaqMan Gene Expression Master Mix from Life Technologies (Carlsbad, CA) on an iQ5 Real-Time PCR machine (Bio-Rad Laboratories). An eight-point, half-log standard curve was generated for PIM-1 and actin messages using RNA from untreated cells. A linear trend line (with an R^2 value >0.99) was generated by plotting log concentrations of standard *versus* C_t values generated from the real-time PCR reactions. Relative message levels from shRNA-treated samples were calculated on the basis of the standard curve, normalized to actin, and compared to the nontarget shRNA control.

Colony Formation Assay

For shRNA growth experiments, 500 UM-UC-3 cells were seeded in a 12-well plate 48 hours posttransduction and cultured for 8 to 10 days at 37°C in 5% CO_2. Cells were fixed with 4% paraformaldehyde in phosphate-buffered saline (PBS), washed twice with PBS, and stained with a crystal violet solution (1% crystal violet, 10% ethanol in water). Stained cells were washed thrice with water and imaged after drying on a GelCount colony counter (Oxford Optronix Ltd, Oxford, United Kingdom). Total staining intensity per well was determined by lysis of cells with 200 μl of Triton X-100 lysis buffer [1% Triton X-100, 50 mM Tris-HCl (pH 7.4), 150 mM NaCl, and 1 mM EDTA]. Lysates (100 μl) from each well were transferred to a clear 96-well plate, and absorbance at 560 nm was determined on an EnVision microplate reader PerkinElmer (Waltham, MA). IC_{50} values were determined using GraphPad Prism software. For compound-treated T24 and UM-UC-3, cells were seeded and stained as above but were incubated with various concentrations of TP-3654 or DMSO 1 day after seeding.

Cell Lysis and Western Blots

In all applications, cells were washed with cold PBS and then treated with cell lysis solution (Cell Signaling Technology, Danvers, MA). Lysates were centrifuged at 14,000*g* at 4°C according to the protocol. Protein levels were then measured and normalized using the BCA Protein Assay (Thermo Fisher Scientific, Rockford, IL). Normalized amounts of lysate were then run on precast gels according to the manufacturer protocol, using MOPS running solution (Life Technologies). Gels were transferred using the iBlot system (Life Technologies) and then blocked for 1 hour in a 5% nonfat dry milk TBS-Tween (TBST) solution. Blots were treated with specified antibodies (all provided by Cell Signaling Technology) diluted 1:1000 in 5% BSA-TBST solution separately on a blot shaker overnight at 4°C. Blots were rinsed three times for 5 minutes each after antibody treatments, according to the protocol. The blots were treated with rabbit secondary antibody solutions (Cell Signaling Technology) for 1 hour at room temperature diluted 1:1000 in a 5% nonfat dry milk TBST solution. As with the primary antibodies, the blots were rinsed three times for 5 minutes each before imaging with an enhanced chemiluminescence kit. The blots were stripped and then re-treated overnight with actin when used as a loading control. As explained previously, the blots were treated in antibody solution diluted 1:1000 in 5% BSA-TBST solution overnight. Blots were

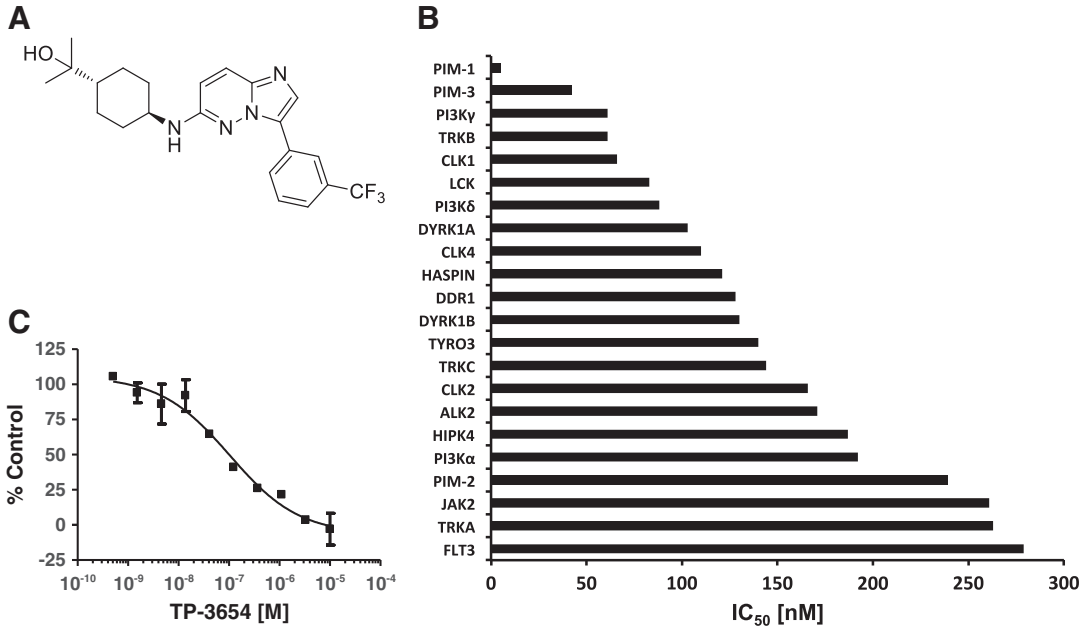

Figure 1. Structure and analysis of TP-3654. (A) TP-3654 compound structure is shown. (B) Selectivity analysis of TP-3654. IC_{50} values are shown for the most potently inhibited kinases. PIM kinase values are K_i values, which were comparable to the IC_{50} determinations. (C) The PIM-1–specific cellular EC_{50} of TP-3654 was determined in a phospho-BAD (S112) Surefire (PerkinElmer, Waltham, MA) assay using HEK-293 cells transfected with BAD and PIM-1. The graph represents data from a single experiment, where the EC_{50} values from four independent experiments (average = 67 nM) were determined using GraphPad Prism software.

treated with mouse secondary antibody (Pierce) and imaged as described previously.

TP-3654 Treatment

UM-UC-3 bladder cancer cells were seeded in six-well plates at a concentration 2.5×10^5 cells per well, allowed to grow for 12 hours, and then treated with 3, 1, 0.3, and 0.03 μM TP-3654 with 0.1% DMSO (vehicle)–treated cells as a negative control. Cells were incubated with the drug for 12 hours and then lysed as described above.

Urothelial Carcinoma Pathology Cases

One hundred thirty-seven cases of urothelial carcinoma were included in this retrospective study of surgical biopsy and resection specimens from the Department of Pathology, University of Utah (Salt Lake City, UT) (retrieved from 2008 to 2011). Tissue was stained with commercially available antibodies against PIM-1, PIM-2, and PIM-3. Cases were classified into three groups according to World Health Organization criteria [invasive high-grade urothelial carcinoma (n = 84), noninvasive high-grade urothelial carcinoma/carcinoma *in situ* (n = 32), and noninvasive low-grade urothelial carcinoma (n = 21)]. Individual cases were reviewed by two of the authors (D.J.A./T.L.) and given a score (0-4) based on a percentage of cells demonstrating positive cytoplasmic and/or nuclear staining for each antibody (<5% = 0; 5%-25% = 1; 26%-50% = 2; 51%-75% = 3; >75% = 4). A score of 2 or greater was considered positive staining.

Table 1. Biochemical*, FLT3†, and hERG‡ Potency Comparison of TP-3654 and SGI-1776

Compound	PIM-1 K_i (nM)	PIM-2 K_i (nM)	PIM-3 K_i (nM)	FLT3 IC_{50} (nM)	hERG IC_{50} (μM)	Molecular Weight
SGI-1776	12	980	20	3	<1	405
TP-3654	5	239	42	279	>30	419

* K_i determined by Reaction Biology as described in the Materials and Methods section.
† FLT3 IC_{50} determined by Reaction Biology as described in the Materials and Methods section.
‡ hERG IC_{50} determined by WuXi AppTec using the QPatch^{HTX} functional hERG assay described in the Materials and Methods section.

Tumor Xenograft Studies

Male and female Nu/Nu mice were purchased from Harlan Sprague Dawley (Indianapolis, IN). Female Nu/Nu mice were used for all xenograft evaluations with the exception of the PC-3 (prostate adenocarcinoma) xenografts where male Nu/Nu mice were used. Cell lines were expanded *in vitro* in complete media and if adherent were harvested by trypsin-EDTA, centrifuged, and resuspended in PBS 1:1 with Matrigel (BD Biosciences, San Jose, CA). Cells were inoculated subcutaneously in the right hind flank of mice. When tumors reached 100 to 200 mm^3 by caliper measurement, mice were randomized, and oral dosing of TP-3654 or vehicle control began and continued every day for 5 days (quaque die [QD] × 5) with 2 days off for 18 to 21 days. Tumor volumes and body weights were determined twice a week, and tumor weights were measured at the completion of the translational xenograft studies.

Pharmacokinetic Study

Female Sprague Dawley® (SD) rats with jugular vein catheters were acquired from Charles River Laboratories (Wilmington, MA) and allowed to acclimate at Tolero's laboratory facility for 3 days. Rats were fasted (no food but with water) for 12 hours before the dosing. Animals (three per group) were dosed with TP-3654 by oral gavage at a dose of 40 mg/kg in a volume of 400 μl per 10 g of body weight. TP-3654 was formulated in a solution of 10% polysorbate 20. Animals dosed IV were heated under a heat lamp before dosing to allow vasodilatation and visualization of the tail vein. These animals

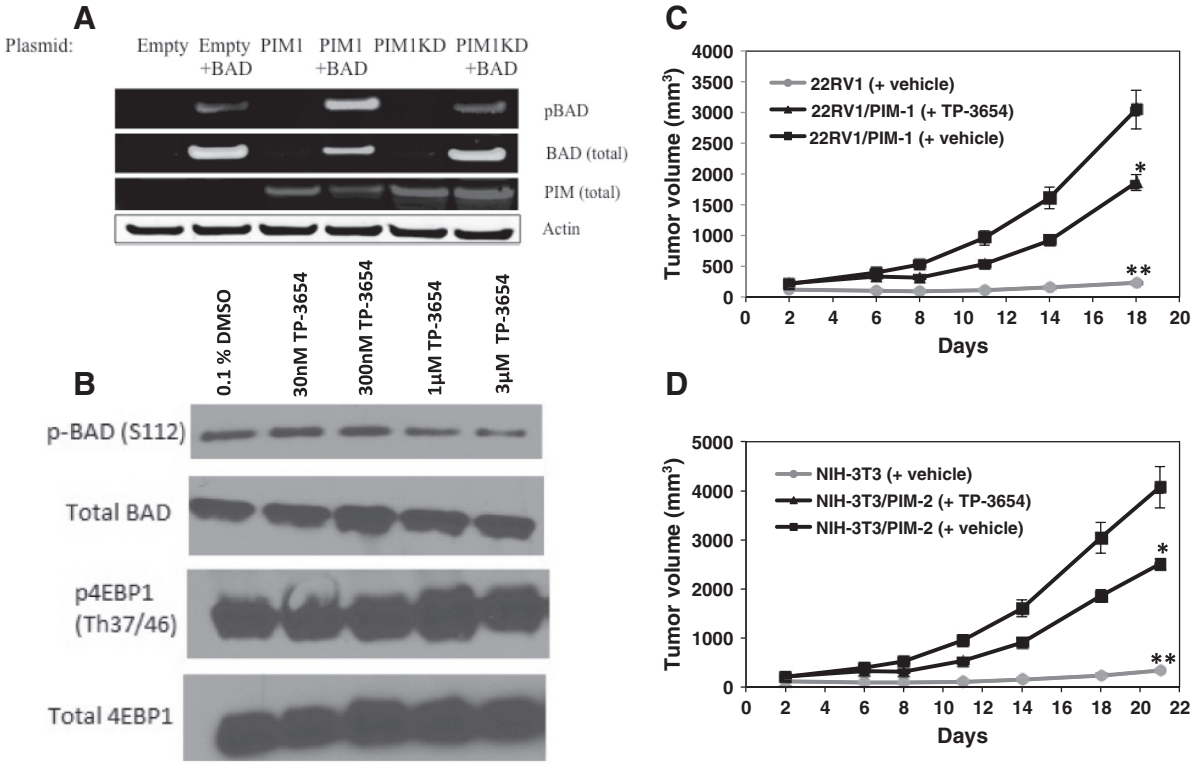

Figure 2. PIM-1 overexpression increases cellular pBAD levels, whereas TP-3654 decreases pBAD levels and PIM-1–driven xenografts. (A) HEK293T cells were transfected with empty vector, PIM1, and PIM1 kinase dead (PIM1KD, K67M) alone or in combination with the PIM substrate BAD using Effectene (Qiagen). Twenty-four hours posttransfection, cells were serum starved overnight and lysed for Western blot detection of phospho-BAD (pBAD) at Ser^{112} using a Li-Cor Odyssey scanner (Lincoln, NE). (B) UM-UC3 cells were treated for 12 hours with 3, 1, 0.3, and 0.03 μM TP-3654. Separate, identical blots were treated with antibodies to measure levels of S112 phosphorylated BAD, total BAD, Th37/46 phosphorylated 4EBP1, and total 4EBP1. (C) Parental 22RV1 and 22RV1/PIM-1 cells (5×10^6) were implanted per Nu/Nu mouse, with 10 mice per group. Mice were dosed by intraperitoneal injection with 25 mg/kg SGI-9481 or vehicle, QD $\times$ 3 weeks, 5 days on 2 days off. Tumor measurements by caliper and body weights (data not shown) were obtained. *P* values for caliper and body weights were $^*P = .023$ and $P = .0002$, respectively. (D) Parental NIH-3 T3 and NIH-3 T3/PIM-2 cells (5×10^6) were implanted per Nu/Nu mouse, with 10 mice per group. Mice were dosed by intraperitoneal injection with 25 mg/kg SGI-9481 or vehicle, QD $\times$ 3 weeks, 5 days on 2 days off. Tumor measurements by caliper and body weights (data not shown) were obtained. *P* values for caliper and body weights were $^*P = .002$ and $P = .0001$, respectively.

were dosed with 2 mg/kg TP-3654 in a volume of 200 μl per 10 g of body weight. After injection, pressure was applied to the site for a few seconds to stop bleeding from the injection. Immediately after each animal received the full dose, time zero began, and blood was collected at the following time points: 1, 5, 25, and 30 minutes and 1, 2, 4, 8, 24, and 48 hours postdose. At the designated time points, an empty 1-ml syringe was used to clear the contents of the jugular vein catheter that had been preloaded with heparin and discarded. A new empty syringe was used to draw 200 μl of whole blood, and the blood was immediately added to EDTA-coated tubes with the appropriate labels. The tubes were gently shaken to ensure that the entire volume of blood interacted with the EDTA to avoid clotting. The collected blood was stored on ice until centrifugation and cryostorage of plasma. A third syringe containing heparin was used to reload the catheter to prevent clotting. After the blood was collected, it was centrifuged at 5000 rpm for 5 minutes at 4°C. The plasma layer was removed and stored at −80°C until extraction and analysis. These steps were repeated until all time points in the study were collected and properly stored. Plasma samples were extracted using standard techniques and analyzed by liquid chromatography-mass spectrometry to quantify TP-3654 concentrations. Pharmacokinetic parameters were determined using the PKSolver add-in program for Excel China Pharmaceutical University (Nanjing, China).

Results

The second-generation PIM kinase inhibitor, TP-3654 (Figure 1*A*), was discovered as a lead candidate on the basis of improved potency against PIM-1 and PIM-2 and no appreciable hERG activity *in vitro* compared to SGI-1776 (Table 1). TP-3654 was tested against a panel of 340 kinases at 1 μM and inhibited 38 kinases by >50% (Appendix A). IC_{50} determinations of 38 protein kinases and 4 additional lipid kinases (PI3K family) revealed 22 kinases with IC_{50} values below 300 nM (Figure 1*B*). TP-3654 displays at least 10-fold or greater selectivity for PIM-1 compared to any other kinase tested. One notable kinase family inhibited by TP-3654 was PI3K (γ, δ, and α), whereas selectivity against FLT3 was reduced by nearly 100-fold relative to SGI-1776 (Table 1).

The cellular potency of TP-3654 was determined by measuring its effect on baseline phosphorylation of BAD, a known substrate of PIM, on serine 112 by overexpression of PIM-1 and BAD in HEK-293 cells. Overexpression of the catalytically inactive mutant PIM-1 (K67M) did not increase phosphorylation of BAD compared to BAD

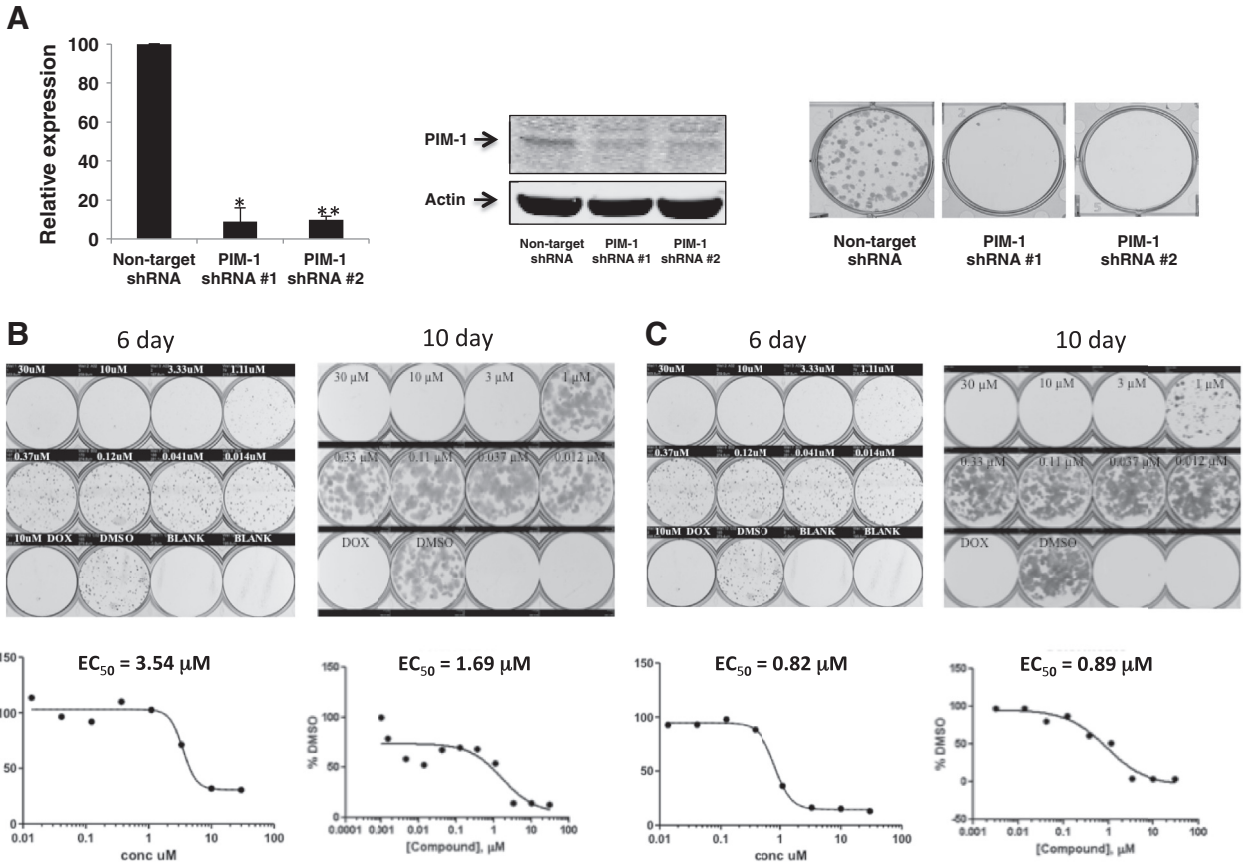

Figure 3. Validation of PIM-1 in solid tumor models *in vitro*. (A) PIM-1 shRNAs or control shRNA (nontarget) was transfected into the UM-UC-3 bladder carcinoma cell line, and PIM-1 mRNA, PIM-1 protein, and cell proliferation in a two dimensional colony formation assay were evaluated. Cells were infected with lentiviral particles overnight, the media were changed, and the cells were collected at 48 hours posttransduction for RNA or protein. A portion of cells were seeded in a six-well plate at 500 cells per well. Cells were fixed and stained after 10 days of growth. Data for PIM-1 mRNA levels are the average (±SD) of two independent experiments, whereas Western blot and colony formation assays are representative of three independent experiments. *P = .0028 and **P = .0002. (B) T24 (bladder) or (C) UM-UC3 (bladder) cancer cell lines were seeded at (B) 300 or (C) 500 cells per well in a 12-well plate and treated the next day with titrated concentrations of TP-3654 as indicated. Cells were grown for 10 or 6 days, respectively, stained for imaging, and lysed for quantitation by absorbance at 560 nm. Data are representative of independent experiments evaluating TP-3654 using T24 and UM-UC3 cell lines, with an average EC_{50} = 1.1 ± 0.4 μM (n = 4) and 2.2 ± 0.2 μM (n = 2), respectively. Colorimetric quantification of cell growth was performed and is provided as the graphs below the respective images with respective EC_{50} values.

transfection alone (Figure 2*A*) and was used as a negative control to subtract BAD phosphorylation by cellular kinases other than PIM-1. TP-3654 demonstrated potent PIM-1 specific cellular activity in the PIM-1/BAD overexpression system with an average EC_{50} = 67 nM (Figure 1*C*). In addition, TP-3654 treatment reduced levels of phospho-BAD *in vitro* using the bladder cancer cell line UM-UC-3 (Figure 2*B*). To exclude the possibility that this phospho-BAD decrease was due to off-target activity, we measured levels of phospho-4EBP1 in parallel with phospho-BAD. We found no appreciable difference in levels of phospho-4EBP1 in TP-3654–treated cells (Figure 2*B*), providing further evidence that PIM inhibition was the primary mechanism for the phospho-BAD decrease observed in TP-3654–treated cells and not activity of the compound inhibiting AKT, another known kinase that can phosphorylate BAD.

In an effort to demonstrate tumorigenicity of the PIM kinases and to evaluate TP-3654 in PIM-driven tumor xenografts, PIM-1– and PIM-2–overexpressing cell lines were developed. The prostate cancer cell line 22RV1 engineered to overexpress PIM-1 as previously described [48] was evaluated *in vivo*. A second model engineered to overexpress PIM-2 was established using the NIH-3 T3 mouse fibroblast cell line. PIM-1 overexpression in 22RV1 cells significantly enhanced subcutaneous tumor growth compared to the parental cell line when grown as mouse xenografts (22RV1 + vehicle *vs* 22RV1/PIM-1 + vehicle), and the growth was significantly reduced by administration of TP-3654 (22RV1/PIM-1 + vehicle *vs* 22RV1/PIM-1 + TP-3654) (Figure 2*C*). No significant changes in body weight were observed in mice from any group. Similarly, PIM-2 overexpression in NIH-3 T3 cells significantly induced subcutaneous tumor growth compared to the parental cell line when grown in mice (NIH-3 T3 + vehicle *vs* NIH-3 T3/PIM-2 + vehicle), and the growth was significantly inhibited by TP-3654 (NIH-3 T3/PIM-2 + vehicle *vs* NIH-3 T3/PIM-2 + TP-3654) (Figure 2*D*). No significant changes in body weight were observed in any group.

The overexpression models extended the observed anti-PIM activity of TP-3654 *in vitro* to antitumor activity *in vivo*. Translational models with more clinical relevance were explored for PIM dependency using shRNA knockdown. The UM-UC-3 urinary epithelial bladder carcinoma cell line was used to verify and validate dependency on

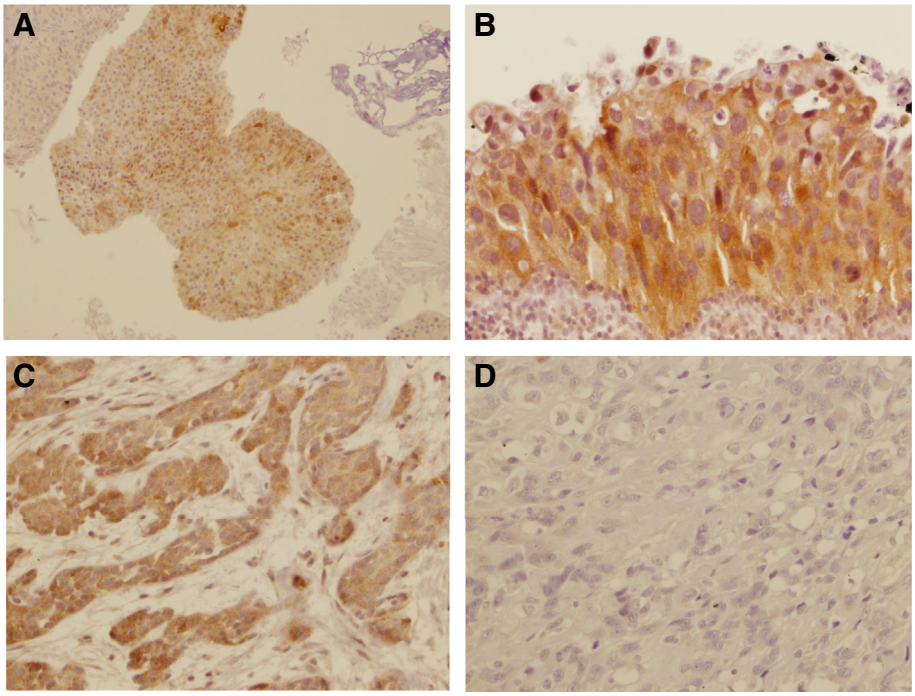

Figure 4. PIM2 kinase expression in urothelial carcinoma cases. (A) Immunohistochemical stained sections of noninvasive low-grade papillary urothelial carcinoma (×200) are shown. (B) Noninvasive high-grade urothelial carcinoma (400×) is shown. (C) Invasive high-grade urothelial carcinoma (×400) is shown. (D) No expression in an invasive high-grade urothelial carcinoma (×400) is shown.

PIM-1 for growth. PIM-1 messenger RNA (mRNA) was significantly reduced using two independent shRNAs targeting PIM-1 compared to the nontarget shRNA control (Figure 3*A*). Furthermore, PIM-1 protein was reduced using PIM-1 shRNA compared to nontarget shRNA, and colony growth in soft agar was markedly reduced with PIM-1 knockdown (Figure 3*A*), comparable to a previous report in the literature [17]. Additionally, TP-3654 reduced colony growth of T24 and UM-UC3 cells (Figure 3, *B* and *C*, respectively), confirming the PIM-1–dependent growth for both cell lines.

Because PIM kinases have been implicated in a number of cancers including hematological and prostate cancers [16,40,41,49–53], we evaluated PIM expression in low, high, noninvasive, and invasive bladder cancer cases. Evaluation of PIM expression by immunohistochemistry revealed a significant number of cases in which PIM was expressed in greater than 25% of the neoplastic cell population (Figure 4 and Table 2). Low-grade noninvasive tumors demonstrated the highest percentage of cases expressing PIM-1 (43%) and PIM-3 (52%), whereas invasive high-grade lesions demonstrated the lowest percentage of PIM-1 (12%) and PIM-3 (13%) staining. PIM-2 was overexpressed in the majority of noninvasive high-grade cases (63%) and in a significant minority of invasive high-grade cases (38%) and noninvasive low-grade cases (33%).

Table 2. PIM Kinase Expression in Urothelial Carcinoma

		PIM-1		PIM-2		PIM-3	
Type	Total *N*	No. (Positive)	%	No. (Positive)	%	No. (Positive)	%
NILG	21	9	43%	7	33%	11	52%
NIHG	32	12	38%	20	63%	9	28%
IHG	84	10	12%	32	38%	11	13%

Number of cases staining positive (scores 2-4) or negative (scores 0-1) in noninvasive low-grade urothelial carcinoma (NILG), noninvasive high-grade urothelial carcinoma (NIHG), and invasive high-grade urothelial carcinoma (IHG).

We next tested whether TP-3654 could inhibit the growth of established mouse xenograft tumors using the UM-UC-3 and PC-3 solid tumor cell lines that were tested *in vitro*. Oral dosing of 200 mg/kg TP-3654 significantly reduced both UM-UC-3 and PC-3 tumor growth measured by volume (caliper) and by final tumor weight, with no significant changes in body weight or gross adverse toxicity (Figure 5).

Previous studies showed that SGI-1776 exhibited favorable pharmacokinetic properties [42], so we determined if TP-3654 retained or possibly improved on the pharmacokinetic parameters of SGI-1776. A pharmacokinetic study in female rats was carried out as described in the Materials and Methods section. Rats were orally dosed with TP-3654 formulated in 10% polysorbate 20 and compared to IV injected control (Figure 6). This formulation showed favorable oral bioavailability at 39%. Using this formulation, the T_{max} for TP-3654 was 1 hour, with a half-life of 4.1 hours (Figure 6).

Discussion

PIM kinases play central roles in tumor cell survival and protection from apoptosis, implicating this family of kinases as valid therapeutic targets [16–19]. To date, numerous inhibitors of PIM kinases that exhibit growth suppressive activity in tumor cell line models *in vitro* and *in vivo* have been generated [9,11,14,33,54–57]. Previous PIM kinase inhibitors demonstrated antitumor activity in xenograft models of *FLT3-ITD* mutant AML and renal cell carcinoma [40,50–53,58]. A recently developed pan-PIM inhibitor has shown promising activity as single agent and in combination with cytarabine in AML xenograft models [59]. Other studies with the same agent have shown promise in multiple myeloma [21]. We have developed a novel small-molecule PIM kinase inhibitor that reduces the growth of solid tumor xenografts where the tumorigenicity is mediated by overexpression of PIM-1 or PIM-2, as well as human bladder carcinoma tumors. Compared to first-generation inhibitor, TP-3654 shows no appreciable hERG activity, suggesting that it would not carry the same cardiotoxic side effects that terminated the phase I trial of SGI-1776.

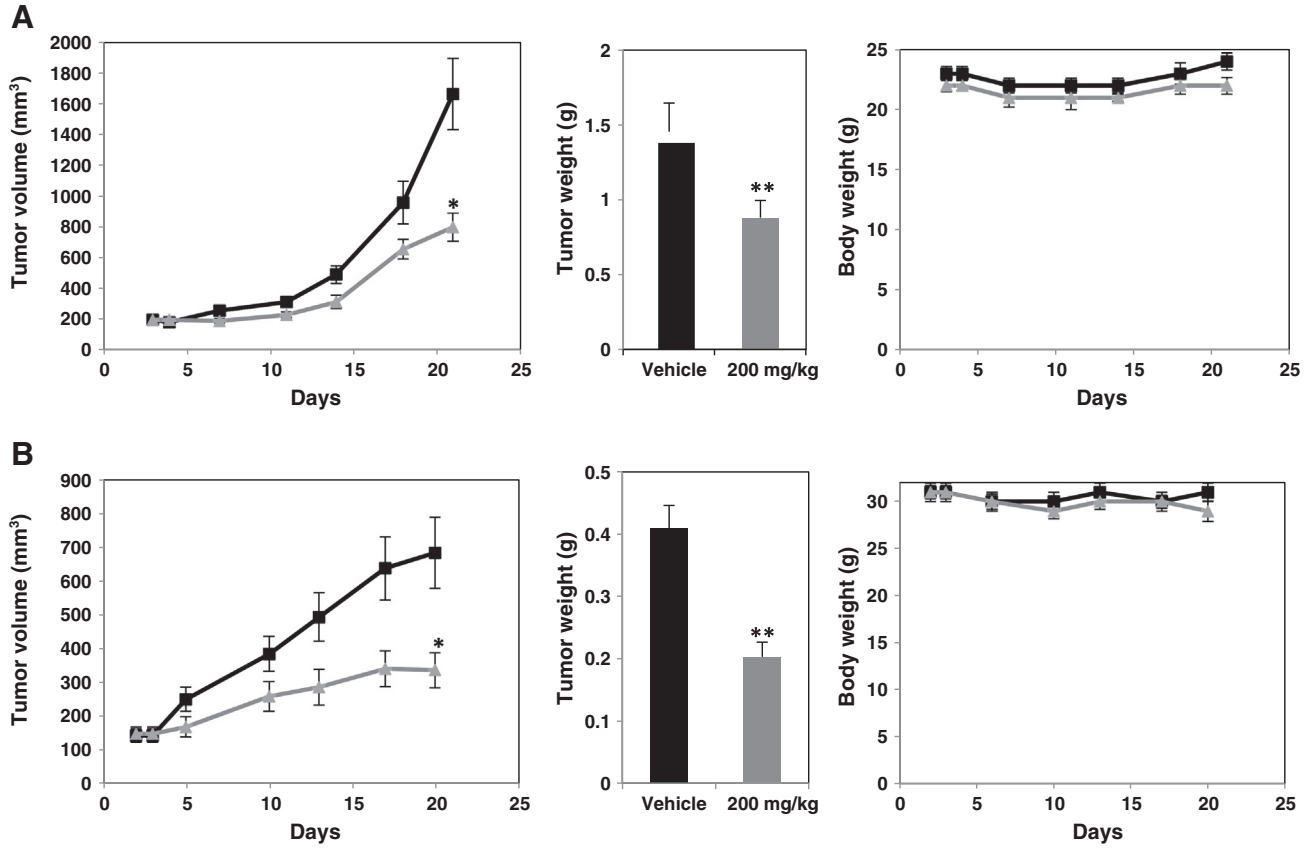

Figure 5. TP-3654 inhibits the growth of established solid tumor xenografts. (A) UM-UC-3 bladder carcinoma cells (5×10^6) were implanted per Nu/Nu mouse, with 12 mice per group. Mice were dosed with TP-3654 orally at 200 mg/kg QD, 3 weeks, 5 days on 2 days off or with vehicle. Caliper measurements (left panel) and tumor weights at the end of the study (middle panel) are shown. No significant change in body weights was observed (right panel). *P = .0028 and **P = .02. (B) PC-3 prostate adenocarcinoma cells (7.5×10^6) were implanted per male Nu/Nu mouse, with 12 mice per group. Mice were dosed with TP-3654 orally at 200 mg/kg QD, 3 weeks, 5 days on 2 days off or with vehicle. Caliper measurements (left panel) and tumor weights at the end of the study (middle panel) are shown. No significant change in body weights was observed (right panel). *P = .007 and **P = .0002.

Although the expression and activity of PIM kinases are well characterized in AML and prostate cancers, we sought to further evaluate the role of PIM kinases in bladder carcinomas. Previous work evaluating bladder carcinoma indicated that PIM-1 was expressed in more than 80% of malignant tissues compared with normal epithelia and that expression was enhanced when comparing specimens derived from patients with bladder cancer with invasive *versus* noninvasive tumors [17]. Furthermore, it was shown that shRNA knockdown of PIM-1 in bladder carcinoma cell lines reduced the growth of the cells *in vitro*, indicating a prominent role for PIM-1 in bladder carcinoma [17]. We evaluated TP-3654 in the bladder cancer model UM-UC-3 *in vitro* and showed that the compound induced similar effects as PIM-1 shRNA-mediated knockdown (compare Figures 2*B* and 3*A*).

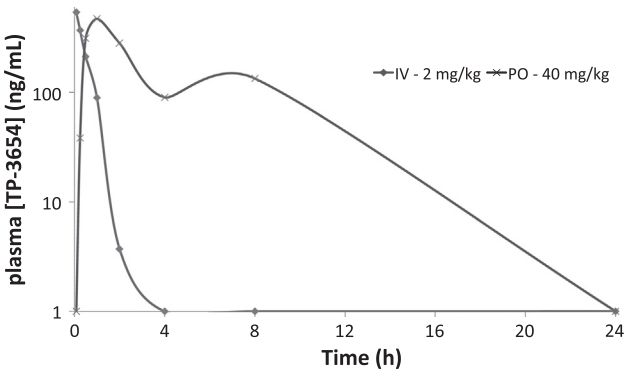

Figure 6. Oral pharmacokinetic data for TP-3654. Plasma levels of TP-3654 (ng/ml) in female SD rats were determined using liquid chromatography-mass spectrometry. Rats were dosed either by IV injection at 2 mg/kg or orally at 40 mg/kg animal body weight. A simple formulation consisting of 10% polysorbate 20 resulted in the highest exposure (or area under the curve) and showed the highest bioavailability when compared to the IV injected animals.

Examination of surgical resection cases of urothelial carcinoma revealed PIM kinases expressed in a significant number of cases when evaluated by immunohistochemistry. There was significant variation across the different groups. Interestingly, PIM-1 and PIM-3 showed a much higher percentage of cases with positive staining in low-grade noninvasive carcinoma compared to invasive high-grade urothelial carcinoma where only a small minority retained positive staining. PIM-2 in comparison was expressed highest in a majority of noninvasive, high-grade lesions and in more than one third of invasive lesions, suggesting that PIM-2 expression remains important in more aggressive clinical disease. These findings suggest that expression of PIM kinases contributes to uncontrolled growth in low- and high-grade noninvasive carcinoma and a smaller number of high-grade invasive tumors.

Superficial, noninvasive urothelial carcinomas are frequently characterized by the mutation of growth factor signaling molecules, whereas the high-grade, more aggressive tumors contain significant loss of tumor suppressor genes [60]. PIM kinase expression is regulated by cytokine signaling, and PIM kinases act as downstream effectors of transcription factors such as c-MYC [61]. PIM kinases also act to inhibit apoptosis by interacting with B cell lymphoma 2 family members such as BAD. Because PIM kinases act as downstream effectors and inhibitors of apoptosis, it is reasonable to expect that they could be expressed in any type of urothelial carcinoma. This hypothesis is consistent with our observation of PIM-1, PIM-2, and PIM- 3 expression in high- and low-grade and invasive and noninvasive urothelial carcinomas. It is unclear why PIM-1 and PIM-3 were predominantly expressed in low-grade, noninvasive tumors, whereas PIM-2 showed higher expression in high-grade tumors. Additional studies on the specific functions of PIM kinases are needed to clarify their roles in the progression of urothelial and other human carcinomas.

The rationale for targeting PIM kinases for the development of cancer therapies includes their overexpression in a variety of malignancies, correlation of high expression levels with poor patient prognosis, their oncogenicity when overexpressed in cells, their role in tumor cell survival as demonstrated by expression knockdown in multiple cancer types, and the development of inhibitors with preclinical activity that are emerging as clinical agents [37,45,59]. Together, these data support the long-standing effort to generate a therapeutic platform from which to target this family of cell survival kinases. Although the initial clinical evaluation of SGI-1776 was halted due to a narrow therapeutic window, the significant potential for therapeutic application of improved drug candidates remains. Given the rapid pace of discovery, optimization, and development of new PIM kinase inhibitors, one or more will likely gain momentum as a potential treatment for both solid and hematologic malignancies, including certain types of urothelial carcinomas.

Supplementary data to this article can be found online at http://dx.doi.org/10.1016/j.neo.2014.05.004.

Acknowledgements

The authors have no additional acknowledgements.

References

[1] Cuypers HT, Selten G, Quint W, Zijlstra M, Maandag ER, Boelens W, van Wezenbeek P, Melief C, and Berns A (1984). Murine leukemia virus-induced T-cell lymphomagenesis: integration of proviruses in a distinct chromosomal region. *Cell* **37**, 141–150.

[2] Meeker TC, Nagarajan L, ar-Rushdi A, Rovera G, Huebner K, and Croce CM (1987). Characterization of the human *PIM-1* gene: a putative proto-oncogene coding for a tissue specific member of the protein kinase family. *Oncogene Res* **1**, 87–101.

[3] Breuer ML, Cuypers HT, and Berns A (1989). Evidence for the involvement of *pim*-2, a new common proviral insertion site, in progression of lymphomas. *EMBO J* **8**, 743–748.

[4] Saris CJ, Domen J, and Berns A (1991). The *pim*-1 oncogene encodes two related protein-serine/threonine kinases by alternative initiation at AUG and CUG. *EMBO J* **10**, 655–664.

[5] Ragoussis J, Senger G, Mockridge I, Sanseau P, Ruddy S, Dudley K, Sheer D, and Trowsdale J (1992). A testis-expressed Zn finger gene (ZNF76) in human 6p21.3 centromeric to the MHC is closely linked to the human homolog of the t-complex gene tcp-11. *Genomics* **14**, 673–679.

[6] Feldman JD, Vician L, Crispino M, Tocco G, Marcheselli VL, Bazan NG, Baudry M, and Herschman HR (1998). KID-1, a protein kinase induced by depolarization in brain. *J Biol Chem* **273**, 16535–16543.

[7] Matikainen S, Sareneva T, Ronni T, Lehtonen A, Koskinen PJ, and Julkunen I (1999). Interferon-alpha activates multiple STAT proteins and upregulates proliferation-associated *IL-2Rα*, *c-myc*, and *pim-1* genes in human T cells. *Blood* **93**, 1980–1991.

[8] Kottaridis PD, Gale RE, Frew ME, Harrison G, Langabeer SE, Belton AA, Walker H, Wheatley K, Bowen DT, and Burnett AK, et al (2001). The presence of a FLT3 internal tandem duplication in patients with acute myeloid leukemia (AML) adds important prognostic information to cytogenetic risk group and response to the first cycle of chemotherapy: analysis of 854 patients from the United Kingdom Medical Research Council AML 10 and 12 trials. *Blood* **98**, 1752–1759.

[9] Mizuno K, Shirogane T, Shinohara A, Iwamatsu A, Hibi M, and Hirano T (2001). Regulation of Pim-1 by Hsp90. *Biochem Biophys Res Commun* **281**, 663–669.

[10] Pasqualucci L, Neumeister P, Goossens T, Nanjangud G, Chaganti RS, Küppers R, and Dalla-Favera R (2001). Hypermutation of multiple proto-oncogenes in B-cell diffuse large-cell lymphomas. *Nature* **412**, 341–346.

[11] Wang Z, Bhattacharya N, Weaver M, Petersen K, Meyer M, Gapter L, and Magnuson NS (2001). Pim-1: a serine/threonine kinase with a role in cell survival, proliferation, differentiation and tumorigenesis. *J Vet Sci* **2**, 167–179.

[12] Mikkers H, Allen J, Knipscheer P, Romeijn L, Hart A, Vink E, and Berns A (2002). High-throughput retroviral tagging to identify components of specific signaling pathways in cancer. *Nat Genet* **32**, 153–159.

[13] Zhu N, Ramirez LM, Lee RL, Magnuson NS, Bishop GA, and Gold MR (2002). CD40 signaling in B cells regulates the expression of the Pim-1 kinase *via* the NF-κB pathway. *J Immunol* **168**, 744–754.

[14] Fox CJ, Hammerman PS, Cinalli RM, Master SR, Chodosh LA, and Thompson CB (2003). The serine/threonine kinase Pim-2 is a transcriptionally regulated apoptotic inhibitor. *Genes Dev* **17**, 1841–1854.

[15] Gaidano G, Pasqualucci L, Capello D, Berra E, Deambrogi C, Rossi D, Maria Larocca L, Gloghini A, Carbone A, and Dalla-Favera R (2003). Aberrant somatic hypermutation in multiple subtypes of AIDS-associated non-Hodgkin lymphoma. *Blood* **102**, 1833–1841.

[16] Fathi AT, Arowojolu O, Swinnen I, Sato T, Rajkhowa T, Small D, Marmsater F, Robinson JE, Gross SD, and Martinson M, et al (2012). A potential therapeutic target for FLT3-ITD AML: PIM1 kinase. *Leuk Res* **36**, 224–231.

[17] Guo S, Mao X, Chen J, Huang B, Jin C, Xu Z, and Qiu S (2010). Overexpression of Pim-1 in bladder cancer. *J Exp Clin Cancer Res* **29**, 161.

[18] Wang J, Anderson PD, Luo W, Gius D, Roh M, and Abdulkadir SA (2012). Pim1 kinase is required to maintain tumorigenicity in MYC-expressing prostate cancer cells. *Oncogene* **31**, 1794–1803.

[19] Beier UH, Weise JB, Laudien M, Sauerwein H, and Görögh T (2007). Overexpression of Pim-1 in head and neck squamous cell carcinomas. *Int J Oncol* **30**, 1381–1387.

[20] Decker S, Finter J, Forde A, Kissel S, Schwaller J, Mack TS, Kuhn A, Gray NS, Follo M, and Jumaa H, et al (2014). PIM kinases are essential for chronic lymphocytic leukemia cell survival (PIM2/3) and CXCR4 mediated microenvironmental interactions (PIM1). *Mol Cancer Ther* **13**, 1231–1245.

[21] Lu J, Zavorotinskaya T, Dai Y, Niu XH, Castillo J, Sim J, Yu J, Wang Y, Langowski JL, and Holash J, et al (2013). Pim2 is required for maintaining multiple myeloma cell growth through modulating TSC2 phosphorylation. *Blood* **122**, 1610–1620.

[22] Gómez-Abad C, Pisonero H, Blanco-Aparicio C, Roncador G, González-Menchén A, Martinez-Climent JA, Mata E, Rodríguez ME, Muñoz-González G, and Sánchez-Beato M, et al (2011). PIM2 inhibition as a rational therapeutic approach in B-cell lymphoma. *Blood* **118**, 5517–5527.

[23] Cibull TL, Jones TD, Li L, Eble JN, Ann Baldridge L, Malott SR, Luo Y, and Cheng L (2006). Overexpression of Pim-1 during progression of prostatic adenocarcinoma. *J Clin Pathol* **59**, 285–288.

[24] Liu HT, Wang N, Wang X, and Li SL (2010). Overexpression of Pim-1 is associated with poor prognosis in patients with esophageal squamous cell carcinoma. *J Surg Oncol* **102**, 683–688.

[25] Warnecke-Eberz U, Bollschweiler E, Drebber U, Metzger R, Baldus SE, Hölscher AH, and Mönig S (2009). Prognostic impact of protein overexpression of the proto-oncogene *PIM-1* in gastric cancer. *Anticancer Res* **29**, 4451–4455.

[26] Yang Q, Chen LS, Neelapu SS, Miranda RN, Medeiros LJ, and Gandhi V (2012). Transcription and translation are primary targets of Pim kinase inhibitor SGI-1776 in mantle cell lymphoma. *Blood* **120**, 3491–3500.

[27] Zippo A, De Robertis A, Serafini R, and Oliviero S (2007). PIM1-dependent phosphorylation of histone H3 at serine 10 is required for MYC-dependent

transcriptional activation and oncogenic transformation. *Nat Cell Biol* **9**, 932–944.
[28] Zhang Y, Wang Z, Li X, and Magnuson NS (2008). Pim kinase-dependent inhibition of c-Myc degradation. *Oncogene* **27**, 4809–4819.
[29] Wang J, Kim J, Roh M, Franco OE, Hayward SW, Wills ML, and Abdulkadir SA (2010). Pim1 kinase synergizes with c-MYC to induce advanced prostate carcinoma. *Oncogene* **29**, 2477–2487.
[30] Magnuson NS, Wang Z, Ding G, and Reeves R (2010). Why target PIM1 for cancer diagnosis and treatment? *Future Oncol* **6**, 1461–1478.
[31] Wierenga AT, Vellenga E, and Schuringa JJ (2008). Maximal STAT5-induced proliferation and self-renewal at intermediate STAT5 activity levels. *Mol Cell Biol* **28**, 6668–6680.
[32] Beharry Z, Zemskova M, Mahajan S, Zhang F, Ma J, Xia Z, Lilly M, Smith CD, and Kraft AS (2009). Novel benzylidene-thiazolidine-2,4-diones inhibit Pim protein kinase activity and induce cell cycle arrest in leukemia and prostate cancer cells. *Mol Cancer Ther* **8**, 1473–1483.
[33] Bullock AN, Russo S, Amos A, Pagano N, Bregman H, Debreczeni JE, Lee WH, von Delft F, Meggers E, and Knapp S (2009). Crystal structure of the PIM2 kinase in complex with an organoruthenium inhibitor. *PLoS One* **4**, e7112.
[34] Chen LS, Redkar S, Bearss D, Wierda WG, and Gandhi V (2009). Pim kinase inhibitor, SGI-1776, induces apoptosis in chronic lymphocytic leukemia cells. *Blood* **114**, 4150–4157.
[35] Xia Z, Knaak C, Ma J, Beharry ZM, McInnes C, Wang W, Kraft AS, and Smith CD (2009). Synthesis and evaluation of novel inhibitors of Pim-1 and Pim-2 protein kinases. *J Med Chem* **52**, 74–86.
[36] Anizon F, Shtil AA, Danilenko VN, and Moreau P (2010). Fighting tumor cell survival: advances in the design and evaluation of Pim inhibitors. *Curr Med Chem* **17**, 4114–4133.
[37] Brault L, Gasser C, Bracher F, Huber K, Knapp S, and Schwaller J (2010). PIM serine/threonine kinases in the pathogenesis and therapy of hematologic malignancies and solid cancers. *Haematologica* **95**, 1004–1015.
[38] Chang M, Kanwar N, Feng E, Siu A, Liu X, Ma D, and Jongstra J (2010). PIM kinase inhibitors downregulate $STAT3^{Tyr705}$ phosphorylation. *Mol Cancer Ther* **9**, 2478–2487.
[39] Santio NM, Vahakoski RL, Rainio EM, Sandholm JA, Virtanen SS, Prudhomme M, Anizon F, Moreau P, and Koskinen PJ (2010). Pim-selective inhibitor DHPCC-9 reveals Pim kinases as potent stimulators of cancer cell migration and invasion. *Mol Cancer* **9**, 279.
[40] Kelly KR, Espitia CM, Taverna P, Choy G, Padmanabhan S, Nawrocki ST, Giles FJ, and Carew JS (2012). Targeting PIM kinase activity significantly augments the efficacy of cytarabine. *Br J Haematol* **156**, 129–132.
[41] Hospital MA, Green AS, Lacombe C, Mayeux P, Bouscary D, and Tamburini J (2012). The FLT3 and Pim kinases inhibitor SGI-1776 preferentially target FLT3-ITD AML cells. *Blood* **119**, 1791–1792.
[42] Chen LS, Redkar S, Taverna P, Cortes JE, and Gandhi V (2011). Mechanisms of cytotoxicity to Pim kinase inhibitor, SGI-1776, in acute myeloid leukemia. *Blood* **118**, 693–702.
[43] Isaac M, Siu A, and Jongstra J (2011). The oncogenic PIM kinase family regulates drug resistance through multiple mechanisms. *Drug Resist Updat* **14**, 203–211.
[44] Mahalingam D, Espitia CM, Medina EC, Esquivel II JA, Kelly KR, Bearss D, Choy G, Taverna P, Carew JS, and Giles FJ, et al (2011). Targeting PIM kinase enhances the activity of sunitinib in renal cell carcinoma. *Br J Cancer* **105**, 1563–1573.
[45] Nawijn MC, Alendar A, and Berns A (2011). For better or for worse: the role of Pim oncogenes in tumorigenesis. *Nat Rev Cancer* **11**, 23–34.
[46] Nishiguchi GA, Atallah G, Bellamacina C, Burger MT, Ding Y, Feucht PH, Garcia PD, Han W, Klivansky L, and Lindvall M (2011). Discovery of novel 3,5-disubstituted indole derivatives as potent inhibitors of Pim-1, Pim-2, and Pim-3 protein kinases. *Bioorg Med Chem Lett* **21**, 6366–6369.
[47] Siu A, Virtanen C, and Jongstra J (2011). PIM kinase isoform specific regulation of MIG6 expression and EGFR signaling in prostate cancer cells. *Oncotarget* **2**, 1134–1144.
[48] Mumenthaler SM, Ng PY, Hodge A, Bearss D, Berk G, Kanekal S, Redkar S, Taverna P, Agus DB, and Jain A (2009). Pharmacologic inhibition of Pim kinases alters prostate cancer cell growth and resensitizes chemoresistant cells to taxanes. *Mol Cancer Ther* **8**, 2882–2893.
[49] Alvarado Y, Giles FJ, and Swords RT (2012). The PIM kinases in hematological cancers. *Expert Rev Hematol* **5**, 81–96.
[50] Jöhrer K, Obkircher M, Neureiter D, Parteli J, Zelle-Rieser C, Maizner E, Kern J, Hermann M, Hamacher F, and Merkel O, et al (2012). Antimyeloma activity of the sesquiterpene lactone cnicin: impact on Pim-2 kinase as a novel therapeutic target. *J Mol Med* **90**, 681–693.
[51] Song JH and Kraft AS (2012). Pim kinase inhibitors sensitize prostate cancer cells to apoptosis triggered by Bcl-2 family inhibitor ABT-737. *Cancer Res* **72**, 294–303.
[52] Tsuganezawa K, Watanabe H, Parker L, Yuki H, Taruya S, Nakagawa Y, Kamei D, Mori M, Ogawa N, and Tomabechi Y, et al (2012). A novel Pim-1 kinase inhibitor targeting residues that bind the substrate peptide. *J Mol Biol* **417**, 240–252.
[53] Tsuhako AL, Brown DS, Koltun ES, Aay N, Arcalas A, Chan V, Du H, Engst S, Franzini M, and Galan A, et al (2012). The design, synthesis, and biological evaluation of PIM kinase inhibitors. *Bioorg Med Chem Lett* **22**, 3732–3738.
[54] Bullock AN, Debreczeni J, Amos AL, Knapp S, and Turk BE (2005). Structure and substrate specificity of the Pim-1 kinase. *J Biol Chem* **280**, 41675–41682.
[55] Jacobs MD, Black J, Futer O, Swenson L, Hare B, Fleming M, and Saxena K (2005). Pim-1 ligand-bound structures reveal the mechanism of serine/threonine kinase inhibition by LY294002. *J Biol Chem* **280**, 13728–13734.
[56] Shay KP, Wang Z, Xing PX, McKenzie IF, and Magnuson NS (2005). Pim-1 kinase stability is regulated by heat shock proteins and the ubiquitin-proteasome pathway. *Mol Cancer Res* **3**, 170–181.
[57] Holder S, Zemskova M, Zhang C, Tabrizizad M, Bremer R, Neidigh JW, and Lilly MB (2007). Characterization of a potent and selective small-molecule inhibitor of the PIM1 kinase. *Mol Cancer Ther* **6**, 163–172.
[58] Pierre F, Regan CF, Chevrel MC, Siddiqui-Jain A, Macalino D, Streiner N, Drygin D, Haddach M, O'Brien SE, and Rice WG, et al (2012). Novel potent dual inhibitors of CK2 and Pim kinases with antiproliferative activity against cancer cells. *Bioorg Med Chem Lett* **22**, 3327–3331.
[59] Garcia PD, Langowski JL, Wang Y, Chen M, Castillo J, Fanton C, Ison M, Zavorotinskaya T, Dai Y, and Lu J, et al (2014). Pan-PIM kinase inhibition provides a novel therapy for treating hematologic cancers. *Clin Cancer Res* **20**, 1834–1845.
[60] Christopher Y, Thomas DT, editors. Molecular pathogenesis of urothelial carcinoma and the development of novel therapeutic strategies; 2010.
[61] White E (2003). The pims and outs of survival signaling: role for the Pim-2 protein kinase in the suppression of apoptosis by cytokines. *Genes Dev* **17**, 1813–1816.